Journal of Nuclear Materials 296 (2001) 243–248

journal of nuclear materials

www.elsevier.com/locate/jnucmat

Compatibility tests on steels in molten lead and lead–bismuth

C. Fazio [a,*], G. Benamati [a], C. Martini [b], G. Palombarini [b]

[a] *Fusion Division, CR Brasimone, Association ENEA-EURATOM, 40032 Camugnano Bologna, Italy*
[b] *Università di Bologna, Istituto di Metallurgia, v.le Risorgimento 4, 40136 Bologna, Italy*

Abstract

The compatibility of steels with liquid lead and liquid lead–bismuth is a critical issue for the development of accelerator-driven system (ADS). In this work the results of a set of preliminary tests carried out in stagnant molten lead at 737 K and in lead–bismuth at 573, 673 and 749 K are summarised. The tests were conducted for 700, 1200, 1500 and 5000 h. Three steels were tested: two martensitic steels (mod. F82H and MANET II) and one austenitic steel (AISI 316L). The martensitic steels underwent oxidation phenomena at the higher testing temperature, due to oxygen dissolved in the melts. At a lower test temperature (573 K) and higher exposure time (5000 h) the oxidation rate of the martensitic steel seems to be lower and the developed oxide layer protective against liquid metal corrosion. The austenitic steel, in turn, exhibited an acceptable resistance to corrosion–oxidation under the test conditions. © 2001 Elsevier Science B.V. All rights reserved.

1. Introduction

The use of lead and lead alloys, as a primary coolant and spallation target material is one of the most attractive options for the next generation of accelerator-driven systems (ADS) [1]. In the ADS concept protons generated from an accelerator impinge on the liquid metal target and by a spallation process neutrons are generated. These neutrons then are used to burn waste nuclear fuel coming from commercial power plants. Lead and the eutectic lead–bismuth are considered two candidates for the production of spallation neutrons because of their high atomic number, low melting points, low vapour pressure and low parasitic neutron capture. In spite of these favourable features, liquid Pb and liquid Pb–55.5Bi could give rise to corrosion-related problems. Exploratory experiments are in progress to examine liquid Pb and liquid Pb–55.5Bi as potential spallation target materials. A reference research project for the development of an ADS demonstration facility is the DEMO design studied in the Italian company Ansaldo in collaboration with ENEA, INFN and CRS4 [2]. In the DEMO reference design the liquid metal coolant in the core could reach temperatures between 573 and 673 K.

A further project, aimed at studying the eutectic lead–bismuth as a spallation target, using the SINQ facility at PSI (Switzerland), is the MEGAPIE (MEGAwatt Pilot Experiments) [3,4]. It could be foreseen that the temperature of the liquid metal in the MEGAPIE design would be between 473 and 623 K [4].

With regard to corrosion phenomena that could occur in the presence of liquid metal, previous experiments indicate that the surfaces of a Fe–9Cr martensitic steel, exposed to molten lead under oxygen control, up to 3000 h and at 823 K, are oxidised [5]. Similar results were obtained on martensitic steel (mod. F82H) exposed to molten lead saturated by oxygen at 793 K for up to 3700 h [6].

The aim of the present work was to carry out preliminary corrosion tests in stagnant lead and eutectic lead–bismuth at lower temperatures and longer exposure times. The steels tested were the two martensitic steels MANET II and mod. F82H, and the austenitic steel AISI 316L. The selected steels are of interest for the DEMO and MEGAPIE projects, since austenitic steels are considered the most valid candidates for the vessel and in-vessel components, and martensitic steels of the

---

[*] Corresponding author. Tel.: +39-534 801 463; fax: +39-534 801 225.

E-mail address: concetta@netbra.brasimone.enea.it (C. Fazio).

0022-3115/01/$ - see front matter © 2001 Elsevier Science B.V. All rights reserved.
PII: S0022-3115(01)00538-4

9–12 Cr class are considered as a reference material both for the core and for the spallation target. The experiments were conducted in the temperature range of interest for the two projects DEMO and MEGAPIE. The explored temperatures were 573, 673 and 749 K and the exposure times 700, 1200, 1500 and 5000 h.

2. Experimental

2.1. Materials

The composition of the two martensitic steels (mod. F82H and MANET II) and the austenitic steel (AISI 316L) are given in Table 1. Stachow GMbH (Germany) supplied the eutectic Pb–55.5Bi (44.8 wt% Pb and 55.2 wt% Bi) alloy used for the herein-described tests. The alloy contained a few ppm of impurities (Ag – 4; Zn – <0.2; Cu – <0.5; Sb – <3; Sn – 9.5; Mg – <1; Cd – 0.2; Fe – <0.6; Ni – <0.9 wppm).

Lead was supplied by GERLI (Italy) and had the following composition of impurities (wppm): Ag – 21; Zn – 1; Cu – 11; Sb – <11; Sn – <64; Mg – 0.6; Ca – 4; Fe – 4.6; Ni – <3.

2.2. Testing

The compatibility tests were performed by exposing the mod. F82H and AISI 316L steels to molten Pb and molten Pb–55.5Bi and MANET II to molten Pb–55.5Bi at constant temperature (737 ± 10 K in Pb and 573, 673 and 749 K in Pb–55.5Bi) using alumina crucibles, in a glove-box in an argon atmosphere. The specimens were placed in each crucible in contact with about 3 kg of molten lead over 700, 1200, 1500 and 5000 h of immersion time. In Table 2 the testing conditions for each sample are summarised. The temperature was measured by chromel–alumel thermocouples placed into the liquid metal. The molten metal was saturated by oxygen, indicated by the presence of oxides floating on the free surface. Measurements of total oxygen content in the liquid metals by extraction from the melt as CO_2 and determination by an IR sensor, carried out before and after the tests, confirmed that the liquid metals were in all cases saturated by oxygen throughout the test.

After extracting the samples from the melt, some were etched in a solution of hydrogen peroxide:acetic acid:ethyl alcohol (1:1:1) to clean the specimens of residual liquid metal and its oxides. Metallographic examinations of the samples were carried out by optical microscopy (OM), scanning electron microscopy (SEM), electron probe microanalysis (EPMA) and X-ray diffraction analysis (XRD). The XRD patterns were recorded on the surface of the samples after etching in the cleaning solution, using a computer-controlled goniometer (0.02° 2θ step, 1 s counting time) and CoKα

Table 1
Chemical composition of the steels

	C (wt%)	Cr (wt%)	Ni (wt%)	W (wt%)	Mn (wt%)	Mo (wt%)	Si (wt%)	V (wt%)	Ti (wt%)	Nb (wt%)	Ta (wppm)	P (wppm)	S (wppm)	B (wppm)	N (wppm)
AISI 316L	0.02	17.3	12.1	–	1.8	2.31	0.35	–	–	–	20	190	5	9	740
Mod. F82H	0.09	7.8	0.04	2	0.18	–	0.13	0.16	0.01	<0.01	–	40	30	91	60
MANET II	0.11	10.3	0.68	–	0.78	0.61	–	0.20	–	0.14	–	30	–	–	30

Table 2
Testing temperature and exposure of the steels to the two melts

Bath	Pb–55.5Bi T (K)			Pb T (K)
	573	673	749	737
Steel	Exposure (h)			Exposure (h)
AISI 316L	1500	1500	700	700
	5000	5000	1200	1200
MANET II	1500	1500	700	–
	5000	5000	1200	
Mod. F82H	–	–	700	700
			1200	1200

radiation. OM and SEM observation and EPMA measurements, carried out by energy dispersive spectroscopy (EDS), were performed on the sample cross-sections.

3. Results

3.1. Mod. F82H steel

The interaction with the oxygen-saturated, molten Pb and Pb–55.5Bi led to the formation of continuous layers of reaction products on the steel surface. The SEM micrograph of the etched cross-section of the steel tested in Pb–55.5Bi at 749 K for 700 h is reported in Fig. 1. As can be observed in this figure the corrosion products have a double-layer structure. The mod. F82H sample exposed to Pb for 700 h behaves in the same way as the mod. F82H sample exposed to Pb–55.5Bi for 700 h. The corrosion products growing on the samples tested for 1200 h in Pb and Pb–55.5Bi both exhibited a double-layer structure. With regard to the composition of the corrosion products on the four samples, EDS and XRD analyses were performed and from these analyses it could be concluded that the inner layer of the four samples had a composition comparable to the $Fe(Fe_{1-x}, Cr_x)_2O_4$ oxide, and the outer layer was mainly magnetite (Fe_3O_4). Furthermore, in the external layer the presence of lead was detected. This suggests that during the growth of the Me_3O_4 layer, particles of metallic lead were embedded in the outer columnar part of the oxide layer. The columnar morphology of the outer layer was observed also in previous studies on mod. F82H exposed to liquid Pb [6] and it is typical of growth along the direction of the diffusing species.

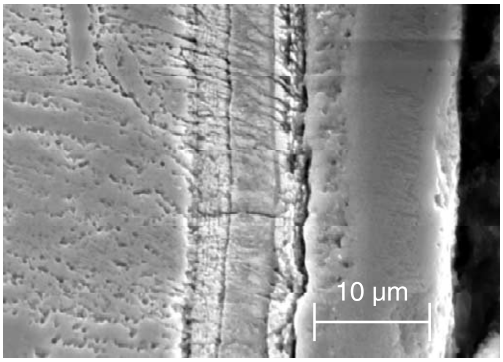

Fig. 1. SEM micrograph, etched cross-section of F82H tested in Pb–55.5Bi at 749 K for 700 h.

The elemental analysis showed that the W content was higher in the inner layer than in the bulk and in the outer layer W was not detected.

The main differences observed in the four samples (two tested in Pb and two in Pb–55.5Bi) were the thickness of the corrosion product layers. The average thickness of the oxide layers measured on the sample immersed for 700 h in Pb was 8 μm, increasing to 20 μm after 1200 h. The thicknesses of the oxide layer on the samples exposed to Pb–55.5Bi were 18 μm after 700 h exposure and 34 μm after 1200 h.

3.2. MANET II steel

After extracting the MANET II samples tested for 1500 h and for 5000 h at 573 K, it could be observed by visual inspection that on the surfaces traces of Pb–55.5Bi alloy were present, while the samples tested for 1500 and 5000 h at 673 K were completely wetted. The MANET II sample exposed to Pb–55.5Bi at 573 K did not suffer corrosive attack and after 5000 h of immersion a very thin oxide scale ($\leqslant 1$ μm) could be observed on the transversal section of the steel (see Fig. 2(a)). At 673 K and after 1500 h an oxide scale could be observed with a thickness of about 1 μm. At the same temperature and after 5000 h exposure the thickness of the oxide scale increased to 5 μm and it was composed of two sublayers, as shown in Fig. 2(b). The composition of the external layer, evaluated by EDS analysis, was comparable to that of Fe_3O_4 and the composition of the inner layer was comparable to the $Fe(Fe_{1-x}, Cr_x)_2O_4$ oxide. Within the oxide scale of the 5000 h tested sample and at the interface with the steel, Pb–55.5Bi was detected. The results of metallographic analyses herein performed

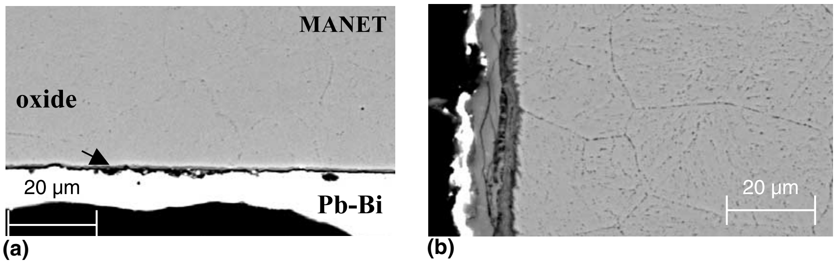

Fig. 2. SEM micrograph, MANET II samples (a) exposed to Pb–55.5Bi at 573 K after 5000 h and (b) exposed to Pb–55.5Bi at 673 K and after 5000 h.

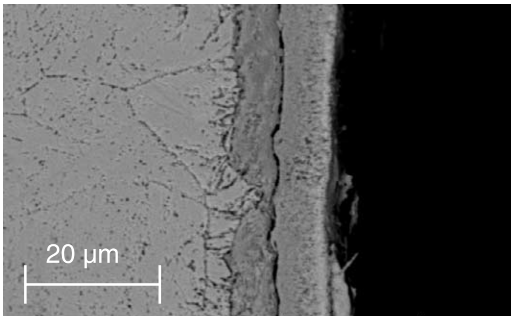

Fig. 3. BSE-image, cross-section of MANET II tested at 749 K for 1200 h in Pb–55.5Bi.

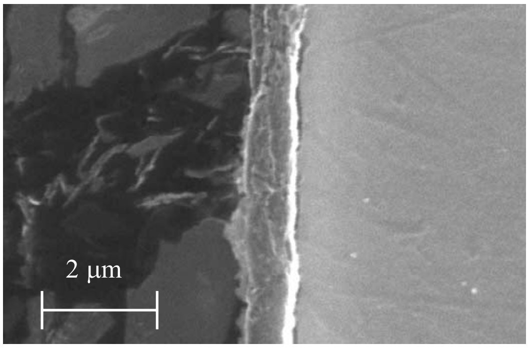

Fig. 4. SEM-micrograph, AISI 316L tested at 573 K in Pb–55.5Bi for 5000 h.

indicate that the presence of the lead alloy at the oxide–steel interface is likely to be due to infiltration of Pb–Bi beneath the scale.

Cross-sections of the MANET II sample tested at 749 K for 1200 h in Pb–55.5Bi are shown in the BSE images of Fig. 3. As can be seen in this figure the edges of both samples corrosion products have a double-layered structure, the same as was observed on the 700 h tested sample. The average thicknesses of the entire oxide layers were 11 µm after 700 h exposure and 16 µm after 1200 h.

EDS analyses and XRD patterns indicate that the inner layer consisted of $Fe(Fe_{1-x},Cr_x)_2O_4$ oxide and the outer layer of Fe_3O_4.

3.3. AISI 316L steel

After extracting the 1500 and 5000 h tested samples from the Pb–55.5Bi bath at 573 K, few traces of the lead alloy could be detected on their surfaces. The lead alloy covered greater areas of the surface samples after 1500 and 5000 h immersion at 673 K. The austenitic steel tested at 573 and 673 K in Pb–55.5Bi for 5000 h exhibited a thin oxide scale ($\leqslant 1$ µm). In Fig. 4 the appearance of the oxide scale detected on the sample tested at 573 K is shown. EDS analysis showed that the scale was mainly composed of Fe, Cr and O. Ni enrichment at the oxide scale–steel interface could be also detected. The corrosion products grown on the surface of the AISI 316 L steel after immersion in Pb at 737 K and in Pb–55.5Bi at 749 K for 1200 h are distributed in a very thin layer on the edge of the surface. Due to the shape of the layers, it was possible to estimate their thickness, which ranged from 2 to 4 µm. As far as the composition of the corrosion products is concerned, several EDS analyses were performed and they indicated that Ni had accumulated at the interface between the corrosion layer and the steel, for both types of melts. The composition of the corrosion products, as confirmed by XRD spectra, corresponds to $Fe(Fe_{1-x},Cr_x)_2O_4$. The same oxide was detected on the samples exposed for 700 h.

4. Discussion

The surface of the AISI 316L and the MANET II steels tested at 573 K for 5000 h in Pb–55.5Bi saturated by oxygen was only partially wetted. From the metallographic analysis it could be observed that neither sample exhibited damage due to corrosive attacks of the lead alloy. On both the steels a very thin ($\leqslant 1$ µm) oxide scale could be observed. The composition of the oxide scale detected on both the steels could be comparable to an $Fe(Fe_{1-x},Cr_x)_2O_4$ oxide. Under the testing conditions the oxide scale acted as a protective barrier against the dissolution of steel alloying elements into the liquid metal. In fact, the mechanism of liquid metal corrosion changes from direct dissolution of the elements to oxidation of the steel surface with increasing dissolved oxygen content in liquid Pb or Pb–55Bi [8]. An adherent and coherent oxide scale effectively protects the steel from corrosion by dissolution, if the thickness of the oxide is stabilised [8].

While at 573 K the oxidation mechanism observed on the two steels seems to be comparable, by increasing the testing temperature to 673 K noticeable differences could be detected. The AISI 316L steel after exposure for 5000 h at 673 K in Pb–55.5Bi still exhibited a thin oxide scale (1 μm) composed of $Fe(Fe_{1-x},Cr_x)_2O_4$ that acted as a barrier against dissolution of alloying elements. On the other hand, the MANET II steel tested in the same conditions exhibited an oxide scale with a thickness of about 5 μm and formed by two layers. The occurrence of stratified oxide layers on martensitic steels was also observed in other works [5,6] and it could be explained on the basis of thermodynamic and kinetic aspects [9,10]. Moreover, for high exposure time the oxide layer exhibited some damage, and infiltration of the alloy through the scale and at the interface with the bulk material was observed. The different behaviour of the two steels could be connected to their different composition (see Table 1): the austenitic steels have a higher oxidation resistance due to the higher Cr content. At 749 K and after 1200 h immersion in Pb–55.5Bi the differences between the AISI 316L and the MANET II steels were more evident. In fact on the austenitic steel the oxide layer detected was 2–4 μm thick and its composition was comparable to that of the $Fe(Fe_{1-x},Cr_x)_2O_4$ oxide. The MANET II steel exhibited a double-layer oxide with a thickness of about 16 μm. In Table 3 is listed the thickness of the oxide layers.

The static tests showed that oxide layers were developed on the austenitic and martensitic steel surfaces. Dynamic tests in oxygen-controlled conditions could give helpful indications in order to evaluate the effectiveness of oxide layers as corrosion barriers.

In comparing the behaviour of the two martensitic steels (F82H and MANET II) exposed to liquid Pb–55.5Bi at 700 and 1200 h it could be seen that on both the steels the corrosion products grew in two main layers: an outer layer with a composition comparable to that of Fe_3O_4 and an inner layer where the Cr content is higher than in the bulk material. The composition of the inner layer corresponds to that of the $Fe(Fe_{1-x},Cr_x)_2O_4$ oxide, in agreement with the results of previous studies [6]. As far as the thickness of the oxide is concerned it was observed that the oxide grown on mod. F82H was thicker than that measured on MANET II. It is probable that the different resistance to oxidation observed on the two martensitic steels could be due to the different Cr content (10.3 wt% for MANET II and 7.8 wt% for mod. F82H). Also the effect on oxide growth of other alloying elements of MANET II steel must be taken into account. In fact, on the basis of oxidation studies on steel in gas phase, it was observed that Nb can increase the oxidation resistance of Fe–Cr alloys [12]. With regard to the other alloying elements in the mod. F82H steel, it was observed that W accumulates in the inner corrosion product layer. A similar phenomenon is described in [7] in which the oxidation of a Fe–4% W alloy causes the accumulation of W in the lower layer of the oxide phases.

Further, it was observed that the corrosion products grown on mod. F82H steel exposed to liquid Pb at 737 K are about 10 μm thinner than those exposed to Pb–55.5Bi at 749 K (see Table 3). These results suggest that liquid Pb–55.5Bi is more oxidising than the liquid Pb. This observation is in agreement to the evaluations performed on the oxygen activity coefficient, which increases with increasing Bi content in the Pb–Bi alloy [11], therefore Pb–Bi is more aggressive than Pb in oxidising conditions.

The AISI 316L specimens tested at 737 K in Pb and at 749 K in Pb–55.5Bi for 1200 h did not exhibit observable differences in terms of thickness of the oxide scales. The composition of the oxide scales, evaluated by SEM–EDS analysis and XRD, corresponds to $Fe(Fe_{1-x},Cr_x)_2O_4$, and accumulation of Ni at the interface between the substrate and the oxide was observed. The enrichment of Ni could be due to the higher affinity of Fe and Cr for oxygen. The mechanism of the

Table 3
Comparison of the measured oxide thickness[a]

Bath/temperature	Pb/737 K		PbBi/573 K		PbBi/673 K		PbBi/749 K	
Exposure (h)	700	1200	1500	5000	1500	5000	700	1200
Steel	Oxide thickness (μm)							
Mod. F82H	8	20	–	–	–	–	18	34
MANET II	–	–	n.m.	$\leqslant 1$	1	5	11	16
AISI 316 L	n.m.	2–4	n.m.	$\leqslant 1$	n.m.	1	n.m.	2–4

[a] n.m. = not measurable.

Ni accumulation is not yet clear and further work is needed to understand it.

5. Conclusions

Preliminary compatibility tests on AISI 316L, MANET II and F82H steels were carried out in stagnant Pb and Pb–55.5Bi, with both melts saturated by oxygen. The testing temperatures and the immersion times are given in Table 2.

At 573 K and after 5000 h immersion in Pb–55.5Bi on the MANET II and the AISI 316L steels an in situ-grown thin oxide scale was detected. It is possible that this oxide scale might act as a protective liquid metal corrosion barrier, even if the steels were not wetted at all.

By increasing the temperature to 673 K, the two steels were wetted and the oxide scale grown on the AISI 316L steel after 5000 h exposure in Pb–55.5Bi seemed to continue to act as an effective corrosion barrier. The oxide observed on MANET II steel, exposed at 673 K for 5000 h, exhibited some damage. The corrosion–oxidation behaviour of AISI 316L and MANET II seemed to be reasonably good in the herein-reported testing conditions but these results have to be validated in flowing liquid alloy.

With regard to the oxidation rate of the martensitic F82H and MANET II steels, it was evident that the Cr content in the steels exposed to liquid Pb (at 737 K) and Pb–55.5Bi (at 749 K), both saturated by oxygen, seemed to be a key parameter. The above-reported evaluations of the oxidation rates in stagnant conditions are limited by the relatively short duration of the tests. The effectiveness of the corrosion barrier should be validated using long-term tests under dynamic conditions.

It is reasonable to suppose that the observed oxidation–corrosion behaviour of the steels in Pb–55.5Bi and in Pb could not be extended to lower oxygen content in the melt and/or to higher temperatures.

Further work is in progress in order to estimate the corrosion–oxidation kinetics of martensitic and austenitic steels under dynamic conditions.

Acknowledgements

The authors wish to thank Mr L. Rapezzi, and Mr M. Guccini for their operations on the glove-box, and the Metallography and Metrology Laboratory of the ENEA centre Brasimone for the metallurgical preparation of the samples.

References

[1] C. Rubbia, J.A. Rubio, S. Buono, F. Carmianti, N. Fìetier, J. Galvez, C. Gelès, Y. Kadi, R. Klapish, P. Mandrillion, J.P. Revol, C. Roche, European Organisation for Nuclear Research, CERN report AT/95-44 (ET), 1995.
[2] L. Cinotti, Doc. ANSALDO, code nr. CIRCE 1 SIEX 0001, 14.1.1999.
[3] M. Salvatores, G.S. Bauer, Executive Outline and Status of the MEGAPIE Initiative, October 1999.
[4] G.S. Bauer, First MEGAPIE General Meeting, Cadarache (France), June 14–15, 2000.
[5] G. Müller, G. Schumacher, F. Zimmermann, J. Nucl. Mater. 278 (2000) 85.
[6] G. Benamati, P. Buttol, V. Imbeni, C. Martini, G. Palombarini, J. Nucl. Mater. 279 (2000) 308.
[7] O. Kubaschewski, B.E. Hopkins, Oxidation of Metals and Alloys, 2nd Ed., Butterworth, London, 1962.
[8] V. Markov, Doc. ENEA VT-SBA-00001 (1997), Seminar on the Concept of Lead-Cooled Fast Reactors, Cadarache (F), September 22–23, 1997 (unpublished).
[9] M. Schütze, in: D.R. Holmes (Ed.), Protective Oxide Scales and Their Breakdown, Wiley, New York, 1997, 2.
[10] ASM Handbook, Corrosion, vol. 13, 1998.
[11] A. Taskinen, Z. Mettalkd. 73 (3) (1982) 163.
[12] F. Armanet, J.H. Davidson, in: P. Lacombe, B. Baroux, G. Béranger (Eds.), Les Editions de Physique, 1990, p. 448.